

Feasible Policy Iteration

Yujie Yang, Zhilong Zheng, Shengbo Eben Li, Jingliang Duan, Jingjing Liu, Xianyuan Zhan, Ya-Qin Zhang

Abstract—Safe reinforcement learning (RL) aims to find the optimal policy and its feasible region in a constrained optimal control problem (OCP). Ensuring feasibility and optimality simultaneously has been a major challenge. Existing methods either attempt to solve OCPs directly with constrained optimization algorithms, leading to unstable training processes and unsatisfactory feasibility, or restrict policies in overly small feasible regions, resulting in excessive conservativeness with sacrificed optimality. To address this challenge, we propose an indirect safe RL framework called feasible policy iteration, which guarantees that the feasible region monotonically expands and converges to the maximum one, and the state-value function monotonically improves and converges to the optimal one. We achieve this by designing a policy update principle called *region-wise policy improvement*, which maximizes the state-value function under the constraint of the constraint decay function (CDF) inside the feasible region and minimizes the CDF outside the feasible region simultaneously. This update scheme ensures that the state-value function monotonically increases state-wise in the feasible region and the CDF monotonically decreases state-wise in the entire state space. Using these two monotonicity properties and the contraction mapping theorem, we prove that the CDF converges to the solution of the risky Bellman equation while the state-value function converges to the solution of the feasible Bellman equation. The former represents the maximum feasible region and the latter manifests the optimal state-value function. Under this framework, we design a practical safe RL algorithm that approximates the CDF using a neural network and optimizes the policy using an interior point method inside the feasible region. Experiments show that our algorithm learns strictly safe and near-optimal policies with accurate feasible regions on classic control tasks. It also achieves fewer constraint violations with performance better than (or comparable to) baselines on Safety Gym.

Index Terms—Safe reinforcement learning, feasibility, optimality, Bellman equation.

1 INTRODUCTION

REINFORCEMENT learning (RL) has achieved promising performance on many challenging tasks such as video games [1], board games [2], robotics [3], and autonomous driving [4]. RL solves an optimal control problem (OCP) by finding a policy that maximizes the expected cumulative rewards. However, in many real-world control tasks, the optimal policy not only needs to maximize rewards but also requires strict safety constraints. Such a problem can be formulated as a constrained OCP. In this paper, we consider stepwise deterministic constraints, which require strict constraint satisfaction at every time step.

In a constrained OCP, every policy has a corresponding safe working area called a ‘feasible region’. The goal of *safe* RL is twofold: finding the optimal policy and its feasible region [5]. Feasibility and optimality are two important prerequisites of a safe RL policy. Feasibility means the constraint is always satisfied under the policy. Optimality means the performance measure (i.e., cumulative rewards) of the policy is optimal. Feasibility and optimality are both

closely related to the size of feasible region. A small feasible region may violate both feasibility and optimality. Feasibility is harmed when an initial state falls outside the feasible region, which results in constraint violations. Optimality is harmed when an optimal state trajectory leaves the feasible region and cannot be reached by the policy. To achieve both feasibility and optimality, we aim to find a policy with the maximum feasible region and the optimal state-value function.

Existing safe RL approaches (*direct* and *indirect* methods) mostly cannot simultaneously ensure feasibility and optimality. Direct methods solve constrained OCPs using constrained optimization algorithms, which suffer from unstable training processes and can result in constant constraint violations while harming feasibility. Indirect methods solve constrained Bellman equations instead of solving constrained OCPs. These methods constrain the policy in overly small feasible regions, which leads to excessive conservativeness and harms optimality.

A widely used algorithm in direct methods is the Lagrange multiplier method, which augments the objective function with constraints using Lagrange multipliers and solves the saddle point of the resulting Lagrange function. For example, Chow et al. [6] constrain the conditional value-at-risk of the cost value function and derive the gradient of the Lagrange function. Tessler et al. [7] learn a single value function to approximate the weighted sum of the reward and the cost signal. Yu et al. [8] learn a Hamilton-Jacobi reachability function and constrain the policy in its reachable set. Yang et al. [9] learn a neural barrier certificate and construct the constraint using a multi-step invariant property. A disadvantage of the Lagrange multiplier method is that its learning process is unstable, i.e., the rewards

- Y. Yang and Z. Zheng contributed equally to this work. All correspondence should be sent to S. E. Li.
- Yujie Yang, Zhilong Zheng, and Shengbo Eben Li are with the School of Vehicle and Mobility, Tsinghua University, Beijing 100084, China. E-mail: yangyj21@mails.tsinghua.edu.cn, zhengzltu@163.com, lisb04@gmail.com.
- Jingliang Duan is with the School of Mechanical Engineering, University of Science and Technology Beijing, Beijing 100083, China. E-mail: duanjl@ustb.edu.cn.
- Jingjing Liu, Xianyuan Zhan, and Ya-Qin Zhang are with the Institute for AI Industry Research, Tsinghua University, Beijing 100084, China. E-mail: jjliu@air.tsinghua.edu.cn, zhanxianyuan@air.tsinghua.edu.cn, zhangyaqin@air.tsinghua.edu.cn.
- This work has been submitted to the IEEE for possible publication. Copyright may be transferred without notice, after which this version may no longer be accessible.

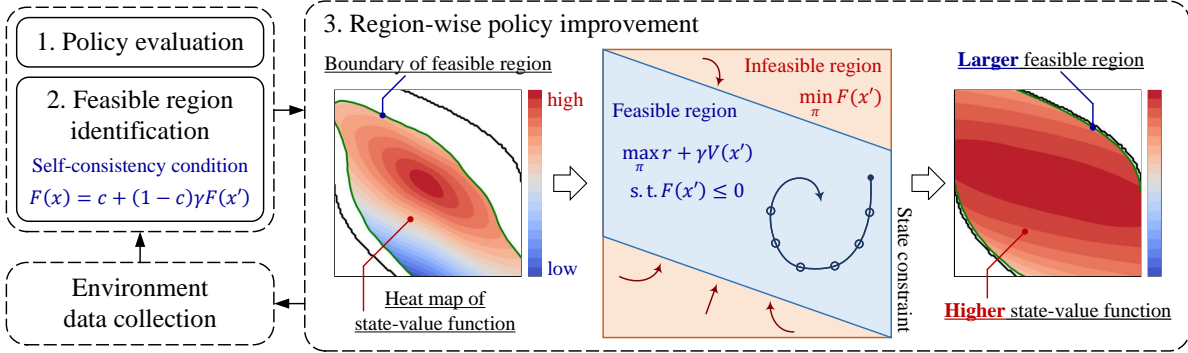


Fig. 1. Feasible policy iteration (FPI). FPI alternately performs policy evaluation, feasible region identification, and region-wise policy improvement. In feasible region identification, we learn a feasibility function using its self-consistency condition. In region-wise policy improvement, we maximize the state-value function under the constraint of the feasibility function inside the feasible region and minimize the feasibility function outside the feasible region. This update rule guarantees a larger feasible region and a higher state-value function. Here, we visualize the feasible region and the state-value function in an adaptive cruise control task. Details of the task can be found in Section 5.1.

and constraint violations oscillate significantly during training [10]. This makes it difficult for the policy to maintain zero constraint violations. The oscillation happens because the Lagrange multiplier method does not provide any guarantee on rewards or constraint violations of intermediate policies. To overcome this, Stooke et al. [10] and Peng et al. [11] use PID control to update the Lagrange multiplier in order to dampen the oscillation. However, theoretical guarantees of intermediate policies are still missing.

Another commonly used direct method is the trust region method, which computes low-order approximations of the objective function and the constraint function, and analytically solves the approximated problems. A representative algorithm of this class is constrained policy optimization (CPO) proposed by Achiam et al. [12]. CPO follows the practice of trust region policy optimization [13], which approximates the objective function with an affine function in a region defined by the policies' KL divergence. CPO further approximates the constraint of the cost value function with an affine function. The authors prove that CPO ensures monotonic policy improvement and near-constraint satisfaction. This improves training stability compared with the Lagrange multiplier method. However, the approximated problem in CPO can become infeasible when there is no policy in the trust region that satisfies the constraint. In this case, CPO performs a recovery update that purely decreases the constraint, which breaks the monotonic policy improvement. Yang et al. [14] deal with this problem by first performing a reward improvement update and then projecting the policy back onto the constrained set. However, their bounds on reward improvement and constraint violation become looser compared to those of CPO and dependent on the constraint violation of the current policy, which can be large at an early stage of training.

Indirect methods do not directly solve the original constrained OCPs but instead solve constrained Bellman equations to obtain solutions for the original OCPs. Existing indirect methods construct constraints of Bellman equations using feasible regions represented by energy functions such as control barrier functions, Lyapunov functions, and safety indexes. Control barrier function (CBF) guarantees control

invariance of its super-level set by requiring that the supremum of its time derivative has a lower bound [15], [16]. Ohnishi et al. [17] propose a barrier-certified adaptive RL algorithm, which constrains the policy in a safe set given by the CBF and optimizes the action-value function in this set. The authors combine CBF with an adaptive model learning algorithm to deal with non-stationary agent dynamics. Ma et al. [18] use a generalized CBF for systems with high relative degrees and mitigate the infeasibility of constrained policy optimization by an adaptive coefficient mechanism.

Lyapunov function ensures forward invariance of its sublevel sets by requiring that its time derivative is always non-positive [19], [20]. Chow et al. [21] construct a Lyapunov function using an auxiliary constraint cost, which is obtained by solving a linear programming problem. The authors propose safe dynamic programming and RL algorithms that constrain the policy search space using the Lyapunov function in policy optimization.

Safety index ensures control invariance in a similar way to CBF [22]. It differs from CBF in that it explicitly considers the relative degree of the system in construction. It adopts a specific functional form, which is a linear combination of the constraint function and its time derivatives. Ma et al. [23] learn a safety index with a given functional form and adjustable parameters by minimizing the occurrence of energy increases. The authors combine the safety index with soft actor-critic [24] and perform a constrained policy update in policy improvement.

A shortcoming of existing indirect methods is that it is difficult to find the maximum feasible region. To ensure constraint satisfaction, they usually construct overly small feasible regions, which impose too strong restrictions on the policy, leading to excessive conservativeness. Some methods obtain feasible regions through learning instead of handcraft design to alleviate this problem [9], [23]. However, these methods rely on the minimization of empirical loss functions, which cannot guarantee convergence to the maximum feasible region.

To address these challenges, we propose an indirect safe RL framework called feasible policy iteration (FPI) that guarantees both feasibility and optimality. We observe that

the feasible region of a policy can be represented by the zero-sublevel set of its feasibility function, which is defined as the aggregation of the infinite-horizon state constraints. FPI uses a feasibility function called the constraint decay function (CDF), which is an exponential function of the number of steps to constraint violation. We design an iteration framework that alternately updates CDF, the state-value function, and the policy, and prove that it converges to the maximum feasible region and the optimal state-value function. Specifically, FPI alternately performs three steps: policy evaluation, feasible region identification, and region-wise policy improvement, as shown in Fig. 1. Policy evaluation and feasible region identification learn the state-value function and the CDF of the current policy respectively. Region-wise policy improvement maximizes the state-value function under the constraint of CDF inside the feasible region and minimizes CDF outside the feasible region.

We prove the convergence of FPI using the monotonicity of region-wise policy improvement plus the Bellman equations of the CDF and the state-value function. By recursively applying the self-consistency condition, we prove that CDF monotonically decreases state-wise in the entire state space and the state-value function monotonically increases state-wise inside the feasible region. Using the contraction mapping theorem, we prove that CDF converges to the solution of the risky Bellman equation, and that the state-value function converges to the solution of the feasible Bellman equation. The former represents the maximum feasible region and the latter equals to the optimal state-value function.

To deal with infinite state spaces, we also propose a practical safe RL algorithm under this framework by approximating CDF using a neural network and optimizing it via minimizing cross-entropy loss. We observe that in region-wise policy improvement, the constraint inside the feasible region is always satisfied by the current policy. This provides us with an initially feasible solution and allows us to use the interior point method for policy optimization, which ensures the feasibility of all intermediate solutions and therefore preserves the monotonic expansion property of the feasible region. The main contributions of this paper are summarized as follows.

- We propose an indirect safe RL framework, feasible policy iteration (FPI), which finds the optimal policy and the maximum feasible region in a constrained OCP. To the best of our knowledge, this is the first work that ensures feasibility and optimality simultaneously.
- We propose a practical safe RL algorithm under this framework that can easily apply to typical control tasks including regulation, tracking, and navigation and effectively handle infinite state space.
- Experiments across multiple benchmarks demonstrate that our algorithm learns strictly safe and near-optimal policies with accurate feasible regions on classic control tasks. It also achieves fewer constraint violations with performance better than (or comparable to) baselines.

2 PRELIMINARIES

2.1 Problem formulation

We consider a deterministic Markov decision process (MDP) specified by a tuple $(\mathcal{X}, \mathcal{U}, f, r, \gamma, d_{\text{init}})$, where $\mathcal{X} \subseteq \mathbb{R}^n$ is the state space, $\mathcal{U} \subseteq \mathbb{R}^m$ is the action space, $f : \mathcal{X} \times \mathcal{U} \rightarrow \mathcal{X}$ is the dynamics model, $r : \mathcal{X} \times \mathcal{U} \rightarrow \mathbb{R}$ is the reward function, $0 < \gamma < 1$ is the discount factor, and d_{init} is the initial state distribution.

Safety is specified through state constraints, i.e., $h(x) \leq 0$, where $h : \mathcal{X} \rightarrow \mathbb{R}$ is the constraint function. The constrained set is defined as $X_{\text{cstr}} = \{x \in \mathcal{X} | h(x) \leq 0\}$. The complement of it, $\bar{X}_{\text{cstr}} = \mathcal{X} \setminus X_{\text{cstr}}$, contains all the states violating the constraints. Our aim is to find a policy $\pi : \mathcal{X} \rightarrow \mathcal{U}$ that maximizes the expected cumulative rewards under the state constraints,

$$\begin{aligned} \max_{\pi} \quad & \mathbb{E}_{x_0 \sim d_{\text{init}}(x)} \left\{ \sum_{t=0}^{\infty} \gamma^t r(x_t, u_t) \right\}, \\ \text{s.t.} \quad & h(x_t) \leq 0, t = 0, 1, \dots, \infty. \end{aligned} \quad (1)$$

2.2 Feasibility

The constraint function only describes the safety of a state at a single time step. To describe long-term safety, we introduce the concept of feasibility. There are two kinds of feasibility: feasibility of a state and feasibility of a policy, which are defined as follows.

Definition 2.1 (Feasibility of a state).

- 1) A state x is feasible if there exists a policy π , such that all successive states under π satisfy the state constraints, i.e., $\exists \pi, \text{s.t. } h(x_t) \leq 0, t = 0, 1, \dots, \infty$, where $x_0 = x$.
- 2) The maximum feasible region, denoted as X^* , is the set of all feasible states. The infeasible region is $\bar{X}^* = \mathcal{X} \setminus X^*$.

A constrained OCP has a solution if and only if its initial state is feasible. Thus, we require that any initial state sampled from d_{init} is feasible so that problem (1) has a solution. The maximum feasible region is the largest area in which the constraint can be satisfied in an infinite horizon. In the infeasible region, the constraint will inevitably be violated no matter what policy is applied.

Definition 2.2 (Feasibility of a policy).

- 1) A policy π is feasible in a state x if all the successive states under π satisfy the state constraint, i.e., $h(x_t) \leq 0, t = 0, 1, \dots, \infty$, where $x_0 = x$.
- 2) The feasible region of π , denoted as X^π , is the set of all states in which π is feasible. The infeasible region of π is $\bar{X}^\pi = \mathcal{X} \setminus X^\pi$.

The feasibility of a policy tells us whether the policy is safe in an infinite horizon. The feasible region of a policy is the area where the policy can be safely applied. It is by definition a subset of the maximum feasible region. To satisfy the constraints of problem (1), a policy must have a feasible region that contains all initial states. To ensure this, we want to find a policy with the maximum feasible region. Note that finding the maximum feasible region is necessary for ensuring not only feasibility but also optimality. This is because a larger feasible region has a greater probability of containing optimal states, which is a necessary condition for the policy to be optimal.

2.3 Feasibility function

Directly solving problem (1) is difficult because it has an infinite number of constraints. The feasibility function aggregates the awkwardly many constraints into a single one and therefore makes the problem tractable. We define the feasibility function as follows.

Definition 2.3 (Feasibility function). *A function $F^\pi : \mathcal{X} \rightarrow \mathbb{R}$ is a feasibility function of a policy π if $\forall x \in \mathcal{X}$,*

$$F^\pi(x) \leq 0 \iff h(x_t) \leq 0, t = 0, 1, \dots, \infty,$$

where $x_0 = x$ and $x_t, t = 1, \dots, \infty$ are sampled by π .

According to Definition 2.3, the zero-sublevel set of a feasibility function is the feasible region of the corresponding policy, i.e., $\{x \in \mathcal{X} | F^\pi(x) \leq 0\} = \mathcal{X}^\pi$. We can replace the infinite-horizon state constraints in problem (1) with a single constraint on the feasibility function, resulting in the following problem.

$$\begin{aligned} \max_{\pi} \quad & \mathbb{E}_{x_0 \sim d_{\text{init}}(x)} \left\{ \sum_{t=0}^{\infty} \gamma^t r(x_t, u_t) \right\}, \\ \text{s.t.} \quad & F^\pi(x_0) \leq 0. \end{aligned} \quad (2)$$

3 METHODS AND THEORETICAL ANALYSIS

In this section, we propose our indirect safe RL framework called feasible policy iteration (FPI). First, we introduce a feasibility function called the constraint decay function (CDF) and a self-consistency-based algorithm to solve it. Then, we detail the core step of our framework, region-wise policy improvement, and prove the monotonicity properties of the CDF and the state-value function. Finally, we present the overall FPI framework and prove that the CDF and the state-value function converge to the solutions of their corresponding Bellman equations.

3.1 Constraint decay function

Definition 3.1 (Constraint decay function). *The constraint decay function of a policy π , $F^\pi : \mathcal{X} \rightarrow [0, 1]$, is defined as*

$$F^\pi(x) = \gamma^{N^\pi(x)}, \quad (3)$$

where $0 < \gamma < 1$ is the discount factor and $N^\pi(x)$ is the number of time steps to constraint violation starting from x under π .

The constraint decay function (CDF) describes the ‘distance’ from a state to constraint violation in the time domain. The smaller the CDF value of a state, the safer it is in the sense that the state is further away from constraint violation. We can choose an appropriate policy such that the CDF values of all states reach their minimum, which means that all states are as safe as possible. Combining all minimum values into a single CDF, we get the optimal CDF.

Definition 3.2 (Optimal constraint decay function). *The optimal constraint decay function, $F^* : \mathcal{X} \rightarrow \mathbb{R}$, is defined as*

$$F^*(x) = \min_{\pi} F^\pi(x). \quad (4)$$

To justify the choice of CDF to represent the feasible region, we first prove that it is a feasibility function.

Proposition 3.1. *The CDF is a feasibility function.*

Proof. $\forall x \in \mathcal{X}, F^\pi(x) \leq 0 \iff N^\pi(x) = \infty \iff h(x_t) \leq 0, t = 0, 1, \dots, \infty$, where $x_0 = x$ and $x_t, t = 1, \dots, \infty$ are sampled by π . \square

Therefore, the zero-sublevel set of the CDF is the feasible region of the corresponding policy. Since the CDF is non-negative, its zero-sublevel set equals its zero-level set. Thus, $\{x \in \mathcal{X} | F^\pi(x) = 0\} = \mathcal{X}^\pi$. The following proposition tells us that the optimal CDF represents the maximum feasible region.

Proposition 3.2. *The zero-level set of the optimal CDF is the maximum feasible region, i.e., $\{x \in \mathcal{X} | F^*(x) = 0\} = \mathcal{X}^*$.*

Proof. $\forall x \in \mathcal{X}$,

$$\begin{aligned} F^*(x) = 0 &\iff \exists \pi, \text{s.t. } F^\pi(x) = 0 \\ &\iff h(x_t) \leq 0, t = 0, 1, \dots, \infty \\ &\iff x \text{ is feasible,} \end{aligned}$$

where $x_0 = x$ and $x_t, t = 1, \dots, \infty$ are sampled by π . \square

The CDF in Definition 3.1 is similar in form to the safety critic used by Thananjeyan et al. [25]. The difference is that they use the safety critic to estimate the discounted probability of constraint violation, while we use the CDF to represent the feasible region. More importantly, we reveal that there exists an optimal CDF that represents the maximum feasible region and can be solved simultaneously with the optimal state-value function (in Section 3.3), resulting in the optimal solution to the constrained OCP. These findings are not addressed by previous works.

The CDF naturally satisfies a recursive relationship, i.e., the self-consistency condition, which is given by the following theorem.

Theorem 3.1 (Self-consistency condition). *The CDF satisfies the self-consistency condition: $\forall x \in \mathcal{X}$,*

$$F^\pi(x) = c(x) + (1 - c(x))\gamma F^\pi(x'), \quad (5)$$

where $c(x) = \mathbf{1}_{\bar{\mathcal{X}}_{\text{cstr}}}(x)$ and $x' = f(x, \pi(x))$.

Proof. We divide the state space into three sets: $\bar{\mathcal{X}}_{\text{cstr}}$, \mathcal{X}^π , and $\bar{\mathcal{X}}^\pi \cap \mathcal{X}_{\text{cstr}}$. They do not overlap with each other and their union is \mathcal{X} . We prove (5) separately in these three sets.

$\forall x \in \bar{\mathcal{X}}_{\text{cstr}}$, the constraint is already violated, and thus $c(x) = 1$ and $N^\pi(x) = 0$. We have $F^\pi(x) = \gamma^0 = 1 = c(x)$, so (5) holds.

$\forall x \in \mathcal{X}^\pi$, the constraint is not violated and will not be violated in the infinite horizon, which means $c(x) = 0$ and $N^\pi(x) = \infty$. The next state x' is still in \mathcal{X}^π , so $N^\pi(x') = \infty$. We have $F^\pi(x) = \gamma^\infty = 0 = F^\pi(x')$, and thus (5) holds.

$\forall x \in \bar{\mathcal{X}}^\pi \cap \mathcal{X}_{\text{cstr}}$, the constraint is not violated, i.e., $c(x) = 0$, but will be violated in a finite number of steps, which satisfies $N^\pi(x) = N^\pi(x') + 1$. We have $F^\pi(x) = \gamma^{N^\pi(x)} = \gamma \cdot \gamma^{N^\pi(x')} = \gamma F^\pi(x')$, and thus (5) holds.

In conclusion, $\forall x \in \mathcal{X}$, (5) holds. \square

The right-hand side of (5) can be viewed as an operator mapping a function to another and F^π is a fixed point of this mapping. The following theorem tells us that this mapping is a contraction mapping on a complete metric space, and therefore has a unique fixed point.

Theorem 3.2 (Unique fixed point). *Define the constraint decay operator D^π as*

$$(D^\pi F)(x) = c(x) + (1 - c(x))\gamma F(x'). \quad (6)$$

D^π has a unique fixed point.

Proof. Consider the metric space (M, d_∞) with $M = \{F | F : \mathcal{X} \rightarrow [0, 1]\}$ and d_∞ being the uniform metric. First, we prove that (M, d_∞) is a complete metric space. Let $\{F_n\}$ be any Cauchy sequence in M , then

$$\forall \epsilon > 0, \exists N \geq 1, \text{s.t. } \forall m, k \geq N, d_\infty(F_m, F_k) < \epsilon,$$

which means

$$|F_m(x) - F_k(x)| < \epsilon, \forall x \in \mathcal{X}. \quad (*)$$

Hence, for all $x \in \mathcal{X}$, $\{F_n(x)\}$ is a Cauchy sequence in $([0, 1], d_\infty)$, which is a complete space (since $[0, 1]$ is a closed subset of \mathbb{R}). It follows that $\{F_n(x)\}$ is a convergent sequence for all $x \in \mathcal{X}$. Let $F_n(x) \rightarrow F(x) \in [0, 1]$. Apparently, $F \in M$. Hold m and let $k \rightarrow \infty$ in $(*)$, then we have

$$|F_m(x) - F(x)| < \epsilon, \forall x \in \mathcal{X},$$

which is equivalent to

$$d_\infty(F_m, F) < \epsilon.$$

Thus we have $F_n \rightarrow F \in M$, so (M, d_∞) is complete.

Then, we prove that D^π is a contraction mapping on (M, d_∞) . $\forall x \in \mathcal{X}$,

$$\begin{aligned} |D^\pi F_1(x) - D^\pi F_2(x)| &= |(1 - c(x))\gamma(F_1(x') - F_2(x'))| \\ &\leq \gamma|F_1(x') - F_2(x')| \\ &\leq \gamma d_\infty(F_1, F_2). \end{aligned}$$

$$\begin{aligned} d_\infty(D^\pi F_1, D^\pi F_2) &= \sup_x |D^\pi F_1(x) - D^\pi F_2(x)| \\ &\leq \gamma d_\infty(F_1, F_2). \end{aligned}$$

Since $\gamma \in (0, 1)$, D^π is a contraction mapping. According to Banach's fixed-point theorem, D^π has a unique fixed point. \square

Since F^π is a fixed point of D^π , the unique fixed point is F^π . This fixed point can be found by iteratively applying D^π starting from an arbitrary F . This iterative algorithm for solving the CDF is called feasible region identification, as shown in Algorithm 1. According to Banach's fixed-point theorem, F^k converges to F^π , i.e., $\lim_{k \rightarrow \infty} F_k = F^\pi$.

Algorithm 1: Feasible region identification

Input: initial CDF F_0 , policy π .
for each iteration k **do**
 for each state $x \in \mathcal{X}$ **do**
 $| F_{k+1}(x) = c(x) + (1 - c(x))\gamma F_k(f(x, \pi(x)))$;
 end
 end

3.2 Region-wise policy improvement

Region-wise policy improvement is the core step of FPI. The ultimate goal of policy optimization is to find a policy with the maximum feasible region and the optimal state-value function. Based on this goal, we want to expand the feasible region and increase the state-value function to the greatest extent in each policy update. In order to achieve this, we propose a region-wise policy update rule. The region here refers to the feasible region of the policy in the previous iteration, which we denote as π_k . Whether a state is in this region can be checked by the CDF of π_k , i.e., if $F^{\pi_k}(x) = 0$, then $x \in \mathcal{X}^{\pi_k}$. The region-wise update rule is as follows.

Inside the feasible region of π_k , we solve a constrained optimization problem, of which the objective function is the reward of the current step plus the state-value function of the next step as in standard policy iteration, and the constraint is that the CDF of the next step equals zero, i.e., $\forall x \in \mathcal{X}^{\pi_k}$,

$$\begin{aligned} \pi_{k+1}(x) &= \arg \max_u r(x, u) + \gamma V^{\pi_k}(x') \\ \text{s.t. } F^{\pi_k}(x') &= 0. \end{aligned} \quad (7)$$

The constraint in (7) requires that the next state is still in \mathcal{X}^{π_k} .

Outside the feasible region of π_k , we minimize the CDF of the next step without constraints, i.e., $\forall x \in \bar{\mathcal{X}}^{\pi_k}$,

$$\pi_{k+1}(x) = \arg \min_u F^{\pi_k}(x'). \quad (8)$$

Next, we prove that the above update rule results in a larger feasible region and a higher state-value function. To prove state-wise monotonicity properties, we assume that the CDF and the state-value function can be accurately approximated. To analyze the size of the feasible region, we study the relationship of the CDFs of the policies in two adjacent iterations. The following theorem tells us that the CDF of the new policy is not greater than that of the old one.

Theorem 3.3 (Feasibility enhancement). *In a deterministic MDP, the CDF of π_{k+1} is not greater than that of π_k in all states, i.e., $\forall x \in \mathcal{X}, F^{\pi_{k+1}}(x) \leq F^{\pi_k}(x)$.*

Proof. According to (7), $\forall x \in \mathcal{X}^{\pi_k}$,

$$F^{\pi_k}(f(x, \pi_{k+1}(x))) = 0 = F^{\pi_k}(f(x, \pi_k(x))).$$

According to (8), $\forall x \in \bar{\mathcal{X}}^{\pi_k}$,

$$\begin{aligned} F^{\pi_k}(f(x, \pi_{k+1}(x))) &= \min_u F^{\pi_k}(f(x, u)) \\ &\leq F^{\pi_k}(f(x, \pi_k(x))). \end{aligned}$$

Thus, $\forall x \in \mathcal{X}$,

$$\begin{aligned} F^{\pi_k}(x) &= c(x) + (1 - c(x))\gamma F^{\pi_k}(f(x, \pi_k(x))) \\ &\geq c(x) + (1 - c(x))\gamma F^{\pi_k}(f(x, \pi_{k+1}(x))). \end{aligned}$$

Let $\{x_t\}_{t=0}^\infty$ be the state sequence in a trajectory under π_{k+1} , where $x_0 = x$. We denote $c(x_t)$ as c_t for simplicity. We have

$$\begin{aligned}
F^{\pi_k}(x) &\geq c_0 + (1 - c_0)\gamma F^{\pi_k}(x_1) \\
&\geq c_0 + (1 - c_0)\gamma(c_1 + (1 - c_1)\gamma F^{\pi_k}(x_2)) \\
&\vdots \\
&\geq c_0 + \gamma(1 - c_0)c_1 + \gamma^2(1 - c_0)(1 - c_1)c_2 + \dots \\
&= \sum_{t=0}^{\infty} \gamma^t \prod_{s=0}^{t-1} (1 - c_s) c_t \\
&= \gamma^{N^{\pi_{k+1}}(x)} \\
&= F^{\pi_{k+1}}(x).
\end{aligned}$$

□

From the proof of Theorem 3.3, we can see that both (7) and (8) play important roles in ensuring the monotonicity of the CDF. Equation (8) takes a minimization so that the CDF decreases outside the feasible region. Equation (7) constrains the CDF at the value of zero inside the feasible region. Since zero is the lowest value of the CDF, this constraint keeps the CDF from increasing. A corollary of Theorem 3.3 is that the feasible region monotonically expands.

Corollary 3.3.1 (Monotonic expansion). *The feasible region of π_{k+1} is at least as large as that of π_k , i.e., $X^{\pi_k} \subseteq X^{\pi_{k+1}}$.*

Proof. $\forall x \in X^{\pi_k}$, $F^{\pi_{k+1}}(x) \leq F^{\pi_k}(x) = 0$, thus $x \in X^{\pi_{k+1}}$.

□

For the state-value function, we study the change of its value inside the feasible region. The following theorem tells us that the state-value function of the new policy is not lower than of the old one in the feasible region.

Theorem 3.4 (Region-wise policy improvement). *In a deterministic MDP, the state-value function of π_{k+1} is not lower than that of π_k in the feasible region of π_k , i.e., $\forall x \in X^{\pi_k}$, $V^{\pi_{k+1}}(x) \geq V^{\pi_k}(x)$.*

Proof. $\forall x \in X^{\pi_k}$, define $U^{\pi_k}(x) = \{u \in \mathcal{U} | F^{\pi_k}(x') = 0\}$. We have $\pi_k(x) \in U^{\pi_k}(x)$. According to (7), we have $\pi_{k+1}(x) \in U^{\pi_k}(x)$ and

$$\begin{aligned}
V^{\pi_k}(x) &= r(x, \pi_k(x)) + \gamma V^{\pi_k}(f(x, \pi_k(x))) \\
&\leq \max_u r(x, u) + \gamma V^{\pi_k}(f(x, u)) \\
&= r(x, \pi_{k+1}(x)) + \gamma V^{\pi_k}(f(x, \pi_{k+1}(x))).
\end{aligned}$$

Let $\{x_t\}_{t=0}^\infty$ be the state sequence in a trajectory under π_{k+1} , where $x_0 = x$. We denote $r(x_t, \pi_{k+1}(x_t))$ as r_t for simplicity.

$$\begin{aligned}
V^{\pi_k}(x) &\leq r_0 + \gamma V^{\pi_k}(x_1) \\
&\leq r_0 + \gamma r_1 + \gamma^2 V^{\pi_k}(x_2) \\
&\vdots \\
&\leq r_0 + \gamma r_1 + \gamma^2 r_2 + \dots \\
&= \sum_{t=0}^{\infty} \gamma^t r_t \\
&= V^{\pi_{k+1}}(x).
\end{aligned}$$

□

Till now, we have proved two monotonicity properties in region-wise policy improvement: the monotonic decreasing

property of the CDF in the entire state space and the monotonic increasing property of the state-value function in the feasible region. These two properties are crucial for the convergence proof of FPI, which is given in the next subsection.

3.3 Feasible policy iteration

Our proposed algorithm, feasible policy iteration (FPI), alternates three steps: policy evaluation, feasible region identification, and region-wise policy improvement. The policy evaluation step computes the state-value function of the current policy as in standard policy iteration. The pseudo-code of FPI is shown in Algorithm 2. In the rest of this subsection, we prove that FPI converges to a policy with the optimal CDF, which represents the maximum feasible region, and the optimal state-value function. This policy is the optimal solution to the constrained OCP (1).

Algorithm 2: Feasible policy iteration (FPI)

Input: initial policy π_0 .
for each iteration k do
 Compute V^{π_k} using policy evaluation;
 Compute F^{π_k} using feasible region identification;
 for each state $x \in X^{\pi_k}$ do
 $\pi_{k+1}(x) = \arg \max_u r(x, u) + \gamma V^{\pi_k}(x')$,
 s.t. $F^{\pi_k}(x') = 0$;
 end
 for each state $x \in \bar{X}^{\pi_k}$ do
 $\pi_{k+1}(x) = \arg \min_u F^{\pi_k}(x')$;
 end
end

First, we introduce a recursive relationship of the optimal CDF called the risky Bellman equation. This equation is also a necessary and sufficient condition of the optimal CDF, which is stated in the following theorem.

Theorem 3.5 (Risky Bellman equation). *$F : \mathcal{X} \rightarrow \mathbb{R}$ is the optimal CDF if and only if it satisfies the risky Bellman equation: $\forall x \in \mathcal{X}$,*

$$F(x) = c(x) + (1 - c(x))\gamma \min_u F(x'). \quad (9)$$

Proof. First, we prove that the optimal CDF satisfies the risky Bellman equation. We divide the state space into three sets: \bar{X}_{cstr} , X^* , and $\bar{X}^* \cap X_{\text{cstr}}$. $\forall x \in \bar{X}_{\text{cstr}}$, $c(x) = 1$ and $F^*(x) = \gamma^0 = 1$, thus (9) holds. $\forall x \in X^*$, $c(x) = 0$ and $\exists \pi$, s.t. $h(x_t) \leq 0$, $t = 0, 1, \dots, \infty$, where $x_0 = x$. Thus, $F^*(x) = 0$, $F^*(x) = \min_u F^*(x') = 0$, (9) holds. $\forall x \in \bar{X}^* \cap X_{\text{cstr}}$, $c(x) = 0$ and $\exists \pi$, s.t. $F^*(x) = F^*(x)$. Then, $\min_u F^*(x') = \min_u F^*(x') = F^*(f(x, \pi(x)))$. Since $F^*(x) = \gamma F^*(f(x, \pi(x)))$, we have $F^*(x) = \gamma \min_u F^*(x')$, (9) holds. Thus, $\forall x \in \mathcal{X}$, (9) holds.

Then, we prove that the right-hand side of (9) is a contraction mapping under the uniform metric. Define the risky Bellman operator D^* as

$$(D^*F)(x) = c(x) + (1 - c(x))\gamma \min_u F(x').$$

$\forall F_1, F_2$ and $x \in \mathcal{X}$, let $u_1 = \arg \min_u F_1(x'), u_2 = \arg \min_u F_2(x')$, and $x'_1 = f(x, u_1), x'_2 = f(x, u_2)$, then

$$\begin{aligned} D^*F_1(x) - D^*F_2(x) &= (1 - c(x))\gamma(F_1(x'_1) - F_2(x'_2)) \\ &\leq (1 - c(x))\gamma(F_1(x'_2) - F_2(x'_2)). \end{aligned}$$

Similarly, we have

$$D^*F_2(x) - D^*F_1(x) \leq (1 - c(x))\gamma(F_2(x'_1) - F_1(x'_1)).$$

Define

$$\begin{aligned} z(x) &= \max\{|(1 - c(x))\gamma(F_1(x'_2) - F_2(x'_2))|, \\ &\quad |(1 - c(x))\gamma(F_2(x'_1) - F_1(x'_1))|\}. \end{aligned}$$

We have

$$|D^*F_1(x) - D^*F_2(x)| \leq z(x).$$

Since

$$\begin{aligned} z(x) &\leq \gamma \max\{|F_1(x'_2) - F_2(x'_2)|, |F_2(x'_1) - F_1(x'_1)|\} \\ &\leq \gamma d_\infty(F_1, F_2), \end{aligned}$$

we have

$$\begin{aligned} |D^*F_1(x) - D^*F_2(x)| &\leq \gamma d_\infty(F_1, F_2) \\ d_\infty(D^*F_1(x), D^*F_2(x)) &\leq \gamma d_\infty(F_1, F_2). \end{aligned}$$

Thus, D^* is a contraction mapping. Together with the completeness of $(\{F|F : \mathcal{X} \rightarrow [0, 1]\}, d_\infty)$ proved before, according to Banach's fixed-point theorem, D^* has a unique fixed point, which is F^* . Therefore, F^* is the unique solution to the risky Bellman equation. Thus, the risky Bellman equation is a necessary and sufficient condition of the optimal CDF. \square

Then, we define the optimal state-value function under the constraint. We define it in the maximum feasible region instead of the entire state space because the constraint will be violated under any policy in the infeasible region. In this case, the optimality of the policy is meaningless since safety is our priority concern. Moreover, we require that the initial state is in the maximum feasible region, and therefore the state will never leave this region under the optimal policy. Thus, it is sufficient to define the optimal state-value function only in the maximum feasible region.

Definition 3.3 (Optimal state-value function). *The optimal state value function $V^* : \mathcal{X}^* \rightarrow \mathbb{R}$ is defined as*

$$V^*(x) = \max_{\pi \in \Pi^*} V^\pi(x), \quad (10)$$

where Π^* is the set of policies of which the feasible regions equal the maximum feasible region, i.e., $\Pi^* = \{\pi | \mathcal{X}^\pi = \mathcal{X}^*\}$.

The optimal state-value function satisfies a recursive relationship called the feasible Bellman equation. This equation is also a necessary and sufficient condition of the optimal state-value function, which is stated in the following theorem.

Theorem 3.6 (Feasible Bellman equation). *$V : \mathcal{X}^* \rightarrow \mathbb{R}$ is the optimal state-value function if and only if it satisfies the feasible Bellman equation: $\forall x \in \mathcal{X}^*$,*

$$V(x) = \max_{u \in \mathcal{U}^*(x)} r(x, u) + \gamma V(x'), \quad (11)$$

where $\mathcal{U}^*(x)$ is the set of actions that keep the next state in the maximum feasible region, i.e., $\mathcal{U}^*(x) = \{u \in \mathcal{U} | x' \in \mathcal{X}^*\}$.

Proof. First, we prove that the optimal state-value function satisfies the feasible Bellman equation. $\forall x \in \mathcal{X}^*$,

$$\begin{aligned} V^*(x) &= \max_{\pi \in \Pi^*} V^\pi(x) \\ &= \max_{u_t \in \mathcal{U}^*(x_t)} \sum_{t=0}^{\infty} \gamma^t r(x_t, u_t) \\ &= \max_{u \in \mathcal{U}^*(x)} r(x, u) + \max_{u_t \in \mathcal{U}^*(x_t)} \sum_{t=1}^{\infty} \gamma^t r(x_t, u_t) \\ &= \max_{u \in \mathcal{U}^*(x)} r(x, u) + \gamma \max_{\pi \in \Pi^*} V^\pi(x') \\ &= \max_{u \in \mathcal{U}^*(x)} r(x, u) + \gamma V^*(x'). \end{aligned}$$

Then, we prove that the feasible Bellman operator B^* , which is defined as

$$(B^*V)(x) = \max_{u \in \mathcal{U}^*(x)} r(x, u) + \gamma V(x'),$$

has a unique fixed point. Consider a metric space (M, d_∞) with $M = \{V | V : \mathcal{X}^* \rightarrow \mathbb{R}\}$. The proof of its completeness is similar to that of $(\{F | F : \mathcal{X} \rightarrow [0, 1]\}, d_\infty)$ and hence omitted here. We only prove that B^* is a contraction mapping on it. $\forall V_1, V_2 \in M$ and $x \in \mathcal{X}^*$, define

$$\begin{aligned} u_1 &= \arg \max_{u \in \mathcal{U}^*(x)} r(x, u) + \gamma V_1(x'), \\ u_2 &= \arg \max_{u \in \mathcal{U}^*(x)} r(x, u) + \gamma V_2(x'), \end{aligned}$$

and let $r_1 = r(x, u_1), r_2 = r(x, u_2), x'_1 = f(x, u_1), x'_2 = f(x, u_2)$, then

$$\begin{aligned} B^*V_1(x) - B^*V_2(x) &= r_1 + \gamma V_1(x'_1) - (r_2 + \gamma V_2(x'_2)) \\ &\leq r_1 + \gamma V_1(x'_1) - (r_1 + \gamma V_2(x'_1)) \\ &= \gamma(V_1(x'_1) - V_2(x'_1)). \end{aligned}$$

Similarly, we have

$$B^*V_2(x) - B^*V_1(x) \leq \gamma(V_2(x'_2) - V_1(x'_2)).$$

Define

$$z(x) = \max\{|\gamma(V_1(x'_1) - V_2(x'_1))|, |\gamma(V_2(x'_2) - V_1(x'_2))|\}.$$

We have

$$|B^*V_1(x) - B^*V_2(x)| \leq z(x).$$

Since

$$\begin{aligned} z(x) &\leq \gamma \max\{|V_1(x'_1) - V_2(x'_1)|, |V_2(x'_2) - V_1(x'_2)|\} \\ &\leq \gamma d_\infty(V_1, V_2), \end{aligned}$$

we have

$$\begin{aligned} |B^*V_1(x) - B^*V_2(x)| &\leq \gamma d_\infty(V_1, V_2) \\ d_\infty(B^*V_1(x), B^*V_2(x)) &\leq \gamma d_\infty(V_1, V_2). \end{aligned}$$

Thus, B^* is a contraction mapping on (M, d_∞) . According to Banach's fixed-point theorem, B^* has a unique fixed point, which is V^* . Therefore, V^* is the unique solution to the feasible Bellman equation. Thus, the feasible Bellman equation is a necessary and sufficient condition of the optimal state-value function. \square

Till now, we have shown that the risky Bellman equation and the feasible Bellman equation are necessary and sufficient conditions for the optimal CDF and the optimal state-value function respectively. Next, we prove the convergence

of FPI by proving that the CDF and the state-value function converge to the solutions of their corresponding Bellman equations.

Theorem 3.7 (Convergence of FPI). *Suppose at the k -th iteration, $\forall x \in \mathcal{X}$, $F^{\pi_{k+1}}(x) = F^{\pi_k}(x)$, and $\forall x \in \mathcal{X}^*$, $V^{\pi_{k+1}}(x) = V^{\pi_k}(x)$, then $F^{\pi_k} = F^*$ and $V^{\pi_k} = V^*$. Moreover, convergence can be achieved in a finite number of iterations in finite state and action spaces.*

Proof. First, we prove that F^{π_k} is the solution to the risky Bellman equation. According to (7), $\forall x \in \mathcal{X}^{\pi_k}$,

$$F^{\pi_k}(f(x, \pi_{k+1}(x))) = 0 = \min_u F^{\pi_k}(f(x, u)).$$

According to (8), $\forall x \in \bar{\mathcal{X}}^{\pi_k}$,

$$F^{\pi_k}(f(x, \pi_{k+1}(x))) = \min_u F^{\pi_k}(f(x, u)).$$

We have

$$\begin{aligned} F^{\pi_{k+1}}(x) &= c(x) + (1 - c(x))\gamma F^{\pi_{k+1}}(f(x, \pi_{k+1}(x))) \\ &= c(x) + (1 - c(x))\gamma F^{\pi_k}(f(x, \pi_{k+1}(x))) \\ &= c(x) + (1 - c(x))\gamma \min_u F^{\pi_k}(f(x, u)) \\ &= c(x) + (1 - c(x))\gamma \min_u F^{\pi_{k+1}}(f(x, u)). \end{aligned}$$

Thus, $F^{\pi_{k+1}}$ is the solution to the risky Bellman equation. Since $F^{\pi_k} = F^{\pi_{k+1}}$, F^{π_k} is also the solution to the risky Bellman equation.

Next, we prove that V^{π_k} is the solution to the feasible Bellman equation. $\forall x \in \mathcal{X}^*$, define $\mathcal{U}^{\pi_k}(x) = \{u \in \mathcal{U} | F^{\pi_k}(x') = 0\}$. Since $F^{\pi_k} = F^*$, $\mathcal{U}^{\pi_k}(x) = \{u \in \mathcal{U} | x' \in \mathcal{X}^*\} = \mathcal{U}^*(x)$. We have

$$\begin{aligned} V^{\pi_{k+1}}(x) &= r(x, \pi_{k+1}(x)) + \gamma V^{\pi_{k+1}}(f(x, \pi_{k+1}(x))) \\ &= r(x, \pi_{k+1}(x)) + \gamma V^{\pi_k}(f(x, \pi_{k+1}(x))) \\ &= \max_{u \in \mathcal{U}^{\pi_k}(x)} r(x, u) + \gamma V^{\pi_k}(x') \\ &= \max_{u \in \mathcal{U}^*(x)} r(x, u) + \gamma V^{\pi_{k+1}}(x'). \end{aligned}$$

Thus, $V^{\pi_{k+1}}$ is the solution to the feasible Bellman equation. Since $V^{\pi_k} = V^{\pi_{k+1}}$, V^{π_k} is also the solution to the feasible Bellman equation.

Thus, both F^{π_k} and V^{π_k} are optimal, i.e., $F^{\pi_k} = F^*$ and $V^{\pi_k} = V^*$. Because in finite state and action spaces, the number of policies is finite, this process converges to the maximum feasible region and the optimal state-value function in a finite number of iterations. \square

4 PRACTICAL IMPLEMENTATIONS

In this section, we introduce some practical implementations of feasible policy iteration (FPI). We first discuss some techniques when approximating the CDF with a neural network in infinite state spaces. We then show how to combine FPI with a mainstream RL algorithm, soft actor-critic (SAC) [24], to yield a practical safe RL algorithm.

4.1 Approximation of CDF

To deal with infinite state spaces, we use a neural network with a sigmoid output activation function to approximate the CDF. The reason for using a sigmoid activation function is to incorporate the knowledge that the value of CDF is between 0 and 1 into the training process. This makes it easier for the CDF network to converge in practice because it eliminates potential large errors introduced by the bootstrap training method. A problem with the sigmoid activation function is that its gradient is small when the absolute value of the input is large, which slows down the training process. To solve this problem, we use a cross-entropy loss to train the CDF, which applies a logarithm function to the output and magnifies the gradient farther from the origin. In feasible region identification, we optimize the CDF network to approximate the CDF of the current policy. Therefore, we use the right-hand side of the self-consistency condition (5) as the training label. The loss function of the CDF is

$$\begin{aligned} L_F(\phi) &= -\mathbb{E}\{y_F \log F_\phi(x) + (1 - y_F) \log(1 - F_\phi(x))\}, \\ y_F &= c(x) + (1 - c(x))\gamma F_\phi(x'), \end{aligned} \tag{12}$$

where ϕ is the parameter of the CDF network. The output value of the CDF is in $(0, 1)$, so the feasible region cannot be represented by its zero-level set. To deal with this problem, we introduce a feasibility threshold $0 < p < 1$, and use the following two sets,

$$X^F = \{x \in \mathcal{X} | F_\phi(x) < p\}, \quad \bar{X}^F = \{x \in \mathcal{X} | F_\phi(x) \geq p\}, \tag{13}$$

to represent the feasible and infeasible regions, respectively. An explanation for the feasibility threshold is to consider the case where constraint violations can be avoided in an infinite horizon as long as they are avoided in a finite number of steps [26]. Here, the number of steps is $\log_\gamma p$. In this case, the CDF value of any infeasible state must be greater than p . In our experiments, we found that a constant value of 0.1 for p can achieve zero constraint violation on all classic control tasks. In region-wise policy improvement, we solve an inequality-constrained optimization problem in the feasible region, i.e., $\forall x \in X^{\pi_k}$,

$$\begin{aligned} \max_u & r(x, u) + \gamma V^{\pi_k}(x') \\ \text{s.t.} & F^{\pi_k}(x') \leq p. \end{aligned} \tag{14}$$

The initial point of (14), which is the policy from the last iteration, π_k , is a feasible solution, i.e., $F^{\pi_k}(f(x, \pi_k(x))) < p$. This allows us to use the interior point method to solve (14). We add a logarithm barrier function of the constraint to the objective function and remove the constraint,

$$\max_u r(x, u) + \gamma V^{\pi_k}(x) + 1/t \cdot \log(p - F^{\pi_k}(x')). \tag{15}$$

We increase t by a factor every several numbers of iterations, which is a standard practice in the interior point method. As $t \rightarrow \infty$, the solution to (15) approaches the solution to (14). Compared with other constrained optimization methods such as the dual ascent, the advantage of the interior point method is that its intermediate solutions are always feasible regardless of the value of t . This ensures that the monotonic expansion property of the feasible region is preserved. In contrast, the feasibility of solutions in the dual ascent

method is affected by the value of the Lagrange multiplier. It is difficult to find an appropriate Lagrange multiplier that ensures strict feasibility. This is the reason for the oscillating training process of the Lagrange multiplier method.

4.2 Integration with soft actor-critic

We combine FPI with soft actor-critic (SAC) [24] and denote the resulting algorithm as FPI-SAC. It learns an action CDF network G_ϕ , two Q networks $Q_{\omega_1}, Q_{\omega_2}$, and a policy network π_θ . The action CDF G takes the current state and action as input and outputs the CDF value of the next state, i.e., $G(x, u) = F(f(x, u))$. Its loss function is

$$L_G(\phi) = -\mathbb{E}_{(x, u) \sim D} \{y_G \log G_\phi(x, u) + (1 - y_G) \log(1 - G_\phi(x, u))\}, \quad (16)$$

$$y_G = c(x) + (1 - c(x))\gamma G_{\bar{\phi}}(x', u'),$$

where D is the set of transition data collected by the policy and $\bar{\phi}$ is the parameters of the target action CDF network, which is updated slower than the action CDF network for stabilizing the training process. The loss functions of the Q networks are,

$$L_Q(\omega_i) = \mathbb{E}_{(x, u, r, x') \sim D} \{(y_Q - Q_{\omega_i}(x, u))^2\},$$

$$y_Q = r + \gamma \left(\min_{j \in \{1, 2\}} Q_{\bar{\omega}_j}(x', u') - \alpha \log \pi_\theta(u'|x') \right), \quad (17)$$

where $i \in \{1, 2\}$, $\bar{\omega}_j$ are the parameters of the target Q networks, and α is the temperature. The policy loss in a feasible state is

$$l_f(x) = l_r(x) - 1/t \cdot \log(p - G_\phi(x, u)),$$

$$l_r(x) = \alpha \log \pi_\theta(u|x) - \min_{i \in \{1, 2\}} Q_{\omega_i}(x, u),$$

where $u \sim \pi_\theta(\cdot|x)$. The policy loss in an infeasible state is

$$l_i(x) = G_\phi(x, u).$$

The total policy loss is

$$L_\pi(\theta) = \mathbb{E}_{x \sim D} \{m(x)l_f(x) + (1 - m(x))l_i(x)\}, \quad (18)$$

$$m(x) = \mathbf{1}[G_\phi(x, u) < p].$$

The loss function of the temperature is

$$L(\alpha) = \mathbb{E}_{x \sim D} \{-\alpha \log \pi_\theta(u|x) - \alpha \bar{H}\}, \quad (19)$$

where \bar{H} is the target entropy.

5 EXPERIMENTS

We seek to answer the following questions through our experiments:

- 1) Can our proposed FPI framework achieve monotonic feasible region expansion and performance improvement, and eventually converge to the maximum feasible region?
- 2) Compared with those direct algorithms based on the method of Lagrange multipliers and the trust region method, does FPI-SAC demonstrate a more stable during-training performance?
- 3) Does FPI-SAC outperform existing algorithms, including both direct and indirect ones, in terms of both safety and optimality?

With regard to (1), we test our proposed method on four classic control tasks where the dynamics are simple and known, and thus the ground-truth maximum feasible regions are available. To answer (2) and (3), we compare our proposed algorithm with a variety of other algorithms on four high-dimensional robot navigation tasks in Safety Gym [27], which are much more complicated and challenging.

5.1 Environments

We start with task descriptions of the above-mentioned eight environments.

The four classic control tasks include: (1) Adaptive Cruise Control (ACC); (2) Lane Keeping (LK); (3) Pendulum; (4) Quadrotor. The four safety-critical control tasks in Safety Gym [27] include: (1) PointGoal; (2) CarGoal; (3) PointPush; (4) CarPush.

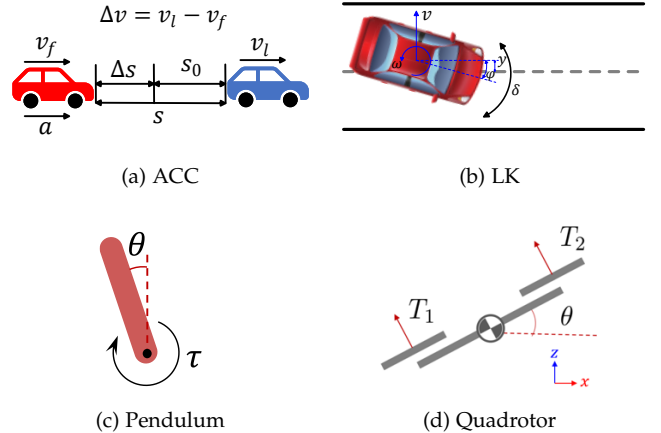


Fig. 2. Schematics of four classic control tasks.

The goal of **ACC** is to control a following vehicle to converge to and maintain a fixed distance with respect to a leading vehicle moving in a uniform motion, as illustrated in Fig. 2(a). **LK** aims to keep a vehicle running in a straight line, i.e., having zero vertical position, yaw angle, lateral velocity, and yaw rate. Fig. 2(b) gives a schematic of this environment. The goal of the **Pendulum** is to apply torque τ on a one-end-fixed pendulum to swing it into an upright position (see Fig. 2(c)). Different to the previous stabilization tasks, the **Quadrotor** is a trajectory tracking task that comes from safe-control-gym [28], where a 2D quadrotor is required to follow a circular trajectory in the vertical plane while keeping the vertical position in a certain range. Fig. 2(d) gives a schematic of this environment. We defer the details of these environments, including the design of their state spaces, action spaces, dynamics, reward functions, and constraints, to the Appendix A.

PointGoal and **CarGoal** are two robot navigation tasks, the aims of which are to control the robot (in red) to reach a goal (in green) while avoiding hazards (in blue), as shown in Fig. 3(a) and 3(b). There are 8 hazards with a radius of 0.2 and a goal with a radius of 0.3. The state includes the velocity of the robot, the position of the goal, and LiDAR point clouds of the hazards. The control inputs of the robots are the torques of their motors, controlling the motion of moving forward and turning for a Point robot, and the left

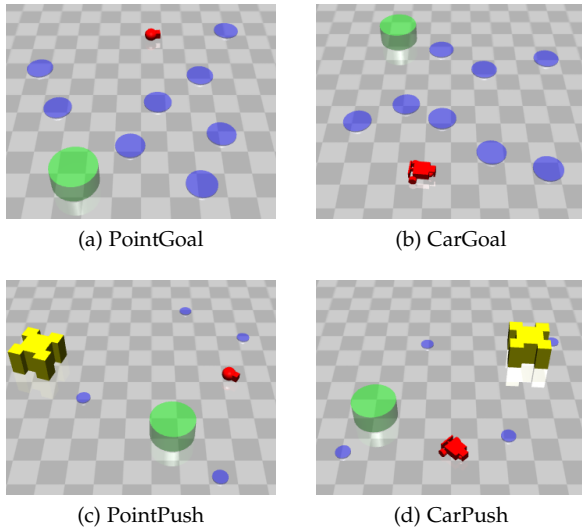


Fig. 3. Snapshots of four Safety Gym tasks.

and right wheels for a Car robot. **PointPush** and **CarPush** are similar to the last two tasks, except that the robots are trying to push a box (in yellow) to the goal, as shown in Fig. 3(c) and 3(d). There are 4 hazards with a radius of 0.1, a goal with a radius of 0.3. The state further includes the position of the box.

5.2 Baselines

The baselines for comparison include both direct and indirect safe RL methods mentioned in Section 1. Regarding the direct methods, we adopt the combinations of Lagrange multipliers method and two mainstream RL algorithms (i.e., SAC and PPO), SAC Lagrangian (**SAC-Lag**) [29] and PPO Lagrangian (**PPO-Lag**) [27], covering both off-policy and on-policy algorithms. The former can be viewed as a Lagrange-based counterpart of FPI-SAC. We also include constrained policy optimization (**CPO**), a representative of the trust-region-based direct methods extending trust region policy optimization [13] to CMDPs. For the indirect methods, we handcraft control barrier functions for all environments and extend SAC with CBF constructing the constraint function, leading to **SAC-CBF**. Details of the CBFs can be found in Appendix B.

5.3 Results

5.3.1 Training curves

The training curves of average episode cost and average episode return, which are the sum of costs and rewards in an episode averaged over multiple episodes, are shown in Fig. 4. Results show that FPI-SAC achieves performance comparable to or higher than baselines while having near-zero constraint violations on all tasks, demonstrating not only low but also stable episode cost curves. SAC-CBF also performs fairly safe, but this comes at the cost of sacrificing optimality, which is the consequence of the overly restrictive constraint. In comparison, the episode cost curves of other algorithms either failed to converge to zero or had severe fluctuation. For example, CPO acts highly unsafely

on LK and all Safety Gym tasks except CarPush, so does SAC-Lag on two Point robot tasks, and PPO-Lag on LK and Quadrotor. These are probably due to the impacts of CPO’s infeasibility problem and the Lagrange multiplier method’s lack of guarantee on constraint satisfaction. Note that although PPO-Lag also performs great on all Safety Gym tasks in terms of safety, its average episode returns on two Point robot tasks are relatively low. Note also how the curves of SAC-Lag and PPO-Lag oscillate or even become worse during training, demonstrating the instability of the Lagrange multiplier method.

5.3.2 Comparison with optimal policy

Since the dynamics of the four classic control tasks are available, we implemented a controller based on Model Predictive Control (MPC), which computes an action sequence in a receding-horizon-control manner. Having access to an accurate model and a long enough prediction horizon, an MPC controller is able to yield an approximately optimal solution. We compare the five algorithms with the MPC controller acting as a performance upper bound.

The evaluation metrics for classic control tasks include constraint violation ratio

$$R_{\text{vio}} = \frac{N_{\text{vio}}}{N} \quad (20)$$

and average normalized return

$$R_{\text{norm}} = \frac{R_{\text{alg}} - R_{\text{base}}}{R_{\text{MPC}} - R_{\text{base}}} - 1, \quad (21)$$

where N_{vio} is the number of episodes where the constraint was violated, and N is the total number of episodes. We uniformly discretize the state space to form a grid of feasible initial states, each point of which yields an episode. R_{alg} , R_{base} and R_{MPC} are the average return across N episodes of a certain algorithm, a random policy and an MPC controller, respectively.

The results of the five algorithms on four classic control tasks are further averaged across three random seeds, as listed in Table 1 in the form of mean \pm standard deviation. Note that we further apply the MPC controller on the four tasks without considering the constraints, so as to show their effectiveness. Results indicate that FPI-SAC achieves zero constraint violation on all four tasks, while all other algorithms violate the constraints on one or more tasks. Meanwhile, FPI-SAC ranks high on all tasks in terms of return, especially ACC and Quadrotor, where FPI-SAC approaches the optimal solutions (The outstanding returns of CPO on ACC come with constraint violation). On the other two tasks, FPI-SAC also achieves comparable returns to the best-performing algorithms.

5.3.3 Visualization

To show the monotonic expansion of the feasible region and monotonic improvement of the state-value function, we take FPI-SAC as an instance and plot some intermediate results during the training, as shown in Fig. 5. The state values are presented as heat maps. The maximum feasible regions and the policy’s feasible regions are outlined with black lines and green lines, respectively. We obtained the maximum

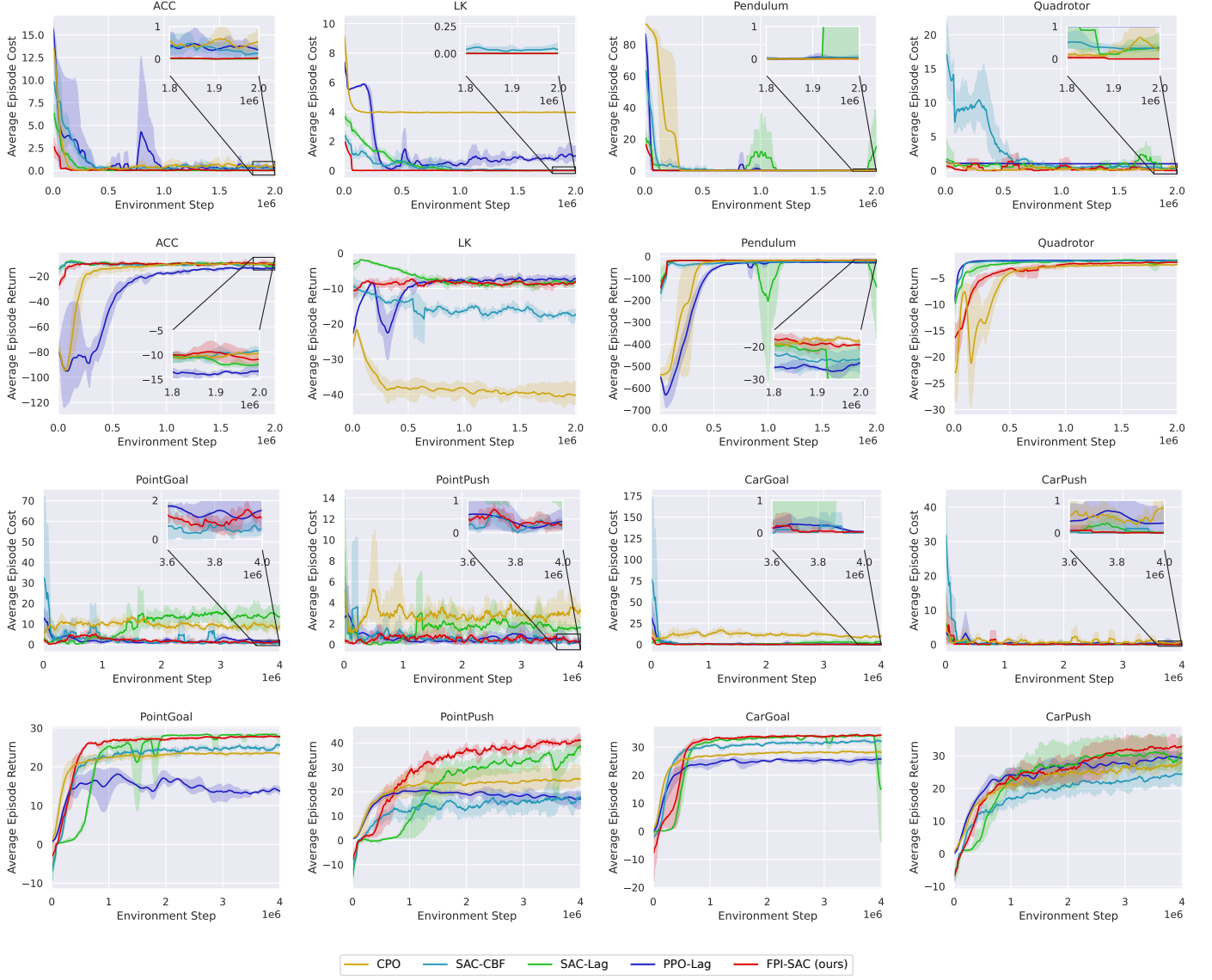


Fig. 4. Training curves on eight environments. The solid line and the shaded region in each figure correspond to the mean and 95% confidence interval over 3 seeds, respectively. For every environment, in the first row are the average episode cost curves, and in the second row are the average episode return curves.

TABLE 1
 R_{vio} and R_{norm} on four classic control tasks.

ACC		LK		Pendulum		Quadrotor		
R_{vio} mean \pm sd(%)	R_{norm} mean \pm sd(%)							
CPO	4.17 \pm 0.00	0.17 \pm 0.14	100.00 \pm 0.00	-17.56 \pm 1.59	0.00 \pm 0.00	-0.04 \pm 0.01	0.00 \pm 0.00	-0.06 \pm 0.01
SAC-Lag	0.00 \pm 0.00	-0.20 \pm 0.17	0.00 \pm 0.00	-0.22 \pm 0.06	0.00 \pm 0.00	-0.59 \pm 0.81	8.89 \pm 3.85	-5.81 \pm 1.55
PPO-Lag	2.78 \pm 2.41	-1.54 \pm 0.44	8.70 \pm 0.00	-0.36 \pm 0.60	2.90 \pm 2.51	-0.62 \pm 0.22	100.00 \pm 0.00	-94.34 \pm 1.37
SAC-CBF	4.17 \pm 0.00	-0.07 \pm 0.05	0.00 \pm 0.00	-3.84 \pm 0.34	8.70 \pm 0.00	-1.34 \pm 1.15	31.11 \pm 6.29	-28.43 \pm 5.37
FPI-SAC (ours)	0.00 \pm 0.00	-0.01 \pm 0.01	0.00 \pm 0.00	-0.25 \pm 0.17	0.00 \pm 0.00	-0.10 \pm 0.02	0.00 \pm 0.00	-0.03 \pm 0.01
MPC w/o cstr.	20.83 \pm 0.00	0.49 \pm 0.00	43.48 \pm 0.00	0.17 \pm 0.00	17.39 \pm 0.00	1.14 \pm 0.00	100.00 \pm 0.00	0.03 \pm 0.00

¹ sd is the abbreviation for standard deviation.

² MPC w/o cstr. means applying an MPC controller without considering the constraint.

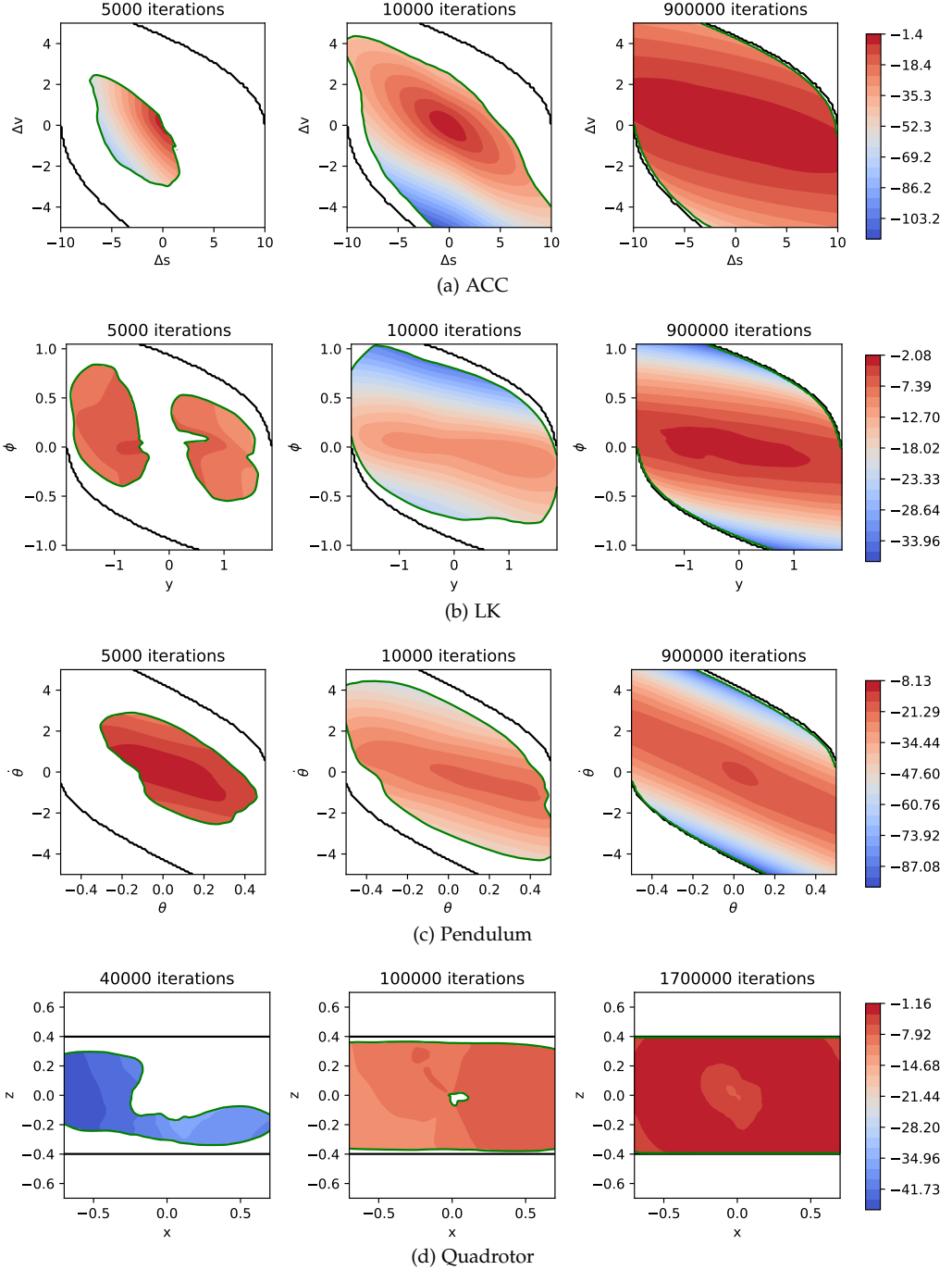


Fig. 5. Heat maps and zero-sublevel sets of the feasibility functions on four classic control tasks. The heat maps correspond to the state values. The black lines are boundaries of the maximum feasible regions, while the green ones around the colored regions are boundaries of zero contours of the feasibility functions.

feasible regions by applying the most conservative, safety-only policy to see if that could reverse the initial constraint-violating tendency. Take ACC as an instance. We use a policy that always takes the maximum deceleration when the initial $\Delta v < 0$ and a policy that always takes the maximum acceleration when the initial $\Delta v > 0$. If the constraint is still violated at the original side, that means the initial state is infeasible, otherwise, it is feasible. In all tasks, FPI-SAC demonstrates monotonicity in terms of both the feasible region and state value, and the feasible regions gradually converge to the maximum feasible regions. Note

that the initial state values in Fig. 5(b) and 5(c) are high only because the value networks are initialized to produce near-zero outputs and haven't acquired to give the true values at this early stage.

6 CONCLUSION

In this paper, we propose an indirect safe RL framework called feasible policy iteration (FPI) that finds the optimal policy and the maximum feasible region in a constrained OCP. The major innovation of FPI is a policy update rule called region-wise policy improvement, which maximizes

the state-value function under the constraint of the CDF inside the feasible region and minimizes the CDF outside the feasible region. This update rule guarantees a monotonic decrease of the CDF and a monotonic increase of the state-value function. We prove that the CDF converges to the solution of the risky Bellman equation and the state-value function converges to the solution of the feasible Bellman equation. The former represents the maximum feasible region and the latter equals the optimal state-value function. We propose a practical safe RL algorithm under the framework of FRI. Experiments show that our algorithm learns strictly safe and near-optimal policies with accurate feasible regions on classic control tasks, and achieves lower constraint violations and performance comparable to or higher than the baselines on Safety Gym.

REFERENCES

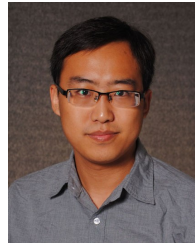
- [1] O. Vinyals, I. Babuschkin, W. M. Czarnecki, M. Mathieu, A. Dudzik, J. Chung, D. H. Choi, R. Powell, T. Ewalds, P. Georgiev *et al.*, "Grandmaster level in starcraft ii using multi-agent reinforcement learning," *Nature*, vol. 575, no. 7782, pp. 350–354, 2019.
- [2] J. Schriftwieser, I. Antonoglou, T. Hubert, K. Simonyan, L. Sifre, S. Schmitt, A. Guez, E. Lockhart, D. Hassabis, T. Graepel, T. Lillicrap, and D. Silver, "Mastering atari, go, chess and shogi by planning with a learned model," *Nature*, vol. 588, no. 7839, pp. 604–609, 2020.
- [3] O. M. Andrychowicz, B. Baker, M. Chociej, R. Jozefowicz, B. McGrew, J. Pachocki, A. Petron, M. Plappert, G. Powell, A. Ray *et al.*, "Learning dexterous in-hand manipulation," *The International Journal of Robotics Research*, vol. 39, no. 1, pp. 3–20, 2020.
- [4] Y. Guan, Y. Ren, Q. Sun, S. E. Li, H. Ma, J. Duan, Y. Dai, and B. Cheng, "Integrated decision and control: Toward interpretable and computationally efficient driving intelligence," *IEEE Transactions on Cybernetics*, pp. 1–15, 2022.
- [5] S. E. Li, *Reinforcement learning for sequential decision and optimal control*. Springer, 2023.
- [6] Y. Chow, M. Ghavamzadeh, L. Janson, and M. Pavone, "Risk-constrained reinforcement learning with percentile risk criteria," *The Journal of Machine Learning Research*, vol. 18, no. 1, pp. 6070–6120, 2017.
- [7] C. Tessler, D. J. Mankowitz, and S. Mannor, "Reward constrained policy optimization," in *International Conference on Learning Representations*, 2019.
- [8] D. Yu, H. Ma, S. Li, and J. Chen, "Reachability constrained reinforcement learning," in *International Conference on Machine Learning*. PMLR, 2022, pp. 25 636–25 655.
- [9] Y. Yang, Y. Jiang, Y. Liu, J. Chen, and S. E. Li, "Model-free safe reinforcement learning through neural barrier certificate," *IEEE Robotics and Automation Letters*, 2023.
- [10] A. Stooke, J. Achiam, and P. Abbeel, "Responsive safety in reinforcement learning by pid lagrangian methods," in *International Conference on Machine Learning*. PMLR, 2020, pp. 9133–9143.
- [11] B. Peng, J. Duan, J. Chen, S. E. Li, G. Xie, C. Zhang, Y. Guan, Y. Mu, and E. Sun, "Model-based chance-constrained reinforcement learning via separated proportional-integral lagrangian," *IEEE Transactions on Neural Networks and Learning Systems*, 2022.
- [12] J. Achiam, D. Held, A. Tamar, and P. Abbeel, "Constrained policy optimization," in *International Conference on Machine Learning*. PMLR, 2017, pp. 22–31.
- [13] J. Schulman, S. Levine, P. Abbeel, M. Jordan, and P. Moritz, "Trust region policy optimization," in *International Conference on Machine Learning*. PMLR, 2015, pp. 1889–1897.
- [14] T.-Y. Yang, J. Rosca, K. Narasimhan, and P. J. Ramadge, "Projection-based constrained policy optimization," in *International Conference on Learning Representations*, 2020.
- [15] A. D. Ames, X. Xu, J. W. Grizzle, and P. Tabuada, "Control barrier function based quadratic programs for safety critical systems," *IEEE Transactions on Automatic Control*, vol. 62, no. 8, pp. 3861–3876, 2016.
- [16] A. D. Ames, S. Coogan, M. Egerstedt, G. Notomista, K. Sreenath, and P. Tabuada, "Control barrier functions: Theory and applications," in *2019 18th European control conference (ECC)*. IEEE, 2019, pp. 3420–3431.
- [17] M. Ohnishi, L. Wang, G. Notomista, and M. Egerstedt, "Barrier-certified adaptive reinforcement learning with applications to brushbot navigation," *IEEE Transactions on robotics*, vol. 35, no. 5, pp. 1186–1205, 2019.
- [18] H. Ma, J. Chen, S. Eben, Z. Lin, Y. Guan, Y. Ren, and S. Zheng, "Model-based constrained reinforcement learning using generalized control barrier function," in *2021 IEEE/RSJ International Conference on Intelligent Robots and Systems (IROS)*. IEEE, 2021, pp. 4552–4559.
- [19] S. M. Richards, F. Berkenkamp, and A. Krause, "The lyapunov neural network: Adaptive stability certification for safe learning of dynamical systems," in *Conference on Robot Learning*. PMLR, 2018, pp. 466–476.
- [20] Y.-C. Chang, N. Roohi, and S. Gao, "Neural lyapunov control," *Advances in neural information processing systems*, vol. 32, 2019.
- [21] Y. Chow, O. Nachum, E. Duenez-Guzman, and M. Ghavamzadeh, "A lyapunov-based approach to safe reinforcement learning," *Advances in neural information processing systems*, vol. 31, 2018.
- [22] C. Liu and M. Tomizuka, "Control in a safe set: Addressing safety in human-robot interactions," in *Dynamic Systems and Control Conference*, vol. 46209. American Society of Mechanical Engineers, 2014, p. V003T42A003.
- [23] H. Ma, C. Liu, S. E. Li, S. Zheng, and J. Chen, "Joint synthesis of safety certificate and safe control policy using constrained reinforcement learning," in *The 4th Annual Learning for Dynamics and Control Conference*, vol. 168. PMLR, 2022, pp. 97–109.
- [24] T. Haarnoja, A. Zhou, P. Abbeel, and S. Levine, "Soft actor-critic: Off-policy maximum entropy deep reinforcement learning with a stochastic actor," in *International conference on machine learning*. PMLR, 2018, pp. 1861–1870.
- [25] B. Thananjeyan, A. Balakrishna, S. Nair, M. Luo, K. Srinivasan, M. Hwang, J. E. Gonzalez, J. Ibarz, C. Finn, and K. Goldberg, "Recovery rl: Safe reinforcement learning with learned recovery zones," *IEEE Robotics and Automation Letters*, vol. 6, no. 3, pp. 4915–4922, 2021.
- [26] G. Thomas, Y. Luo, and T. Ma, "Safe reinforcement learning by imagining the near future," *Advances in Neural Information Processing Systems*, vol. 34, pp. 13 859–13 869, 2021.
- [27] A. Ray, J. Achiam, and D. Amodei, "Benchmarking safe exploration in deep reinforcement learning," *arXiv preprint arXiv:1910.01708*, vol. 7, p. 1, 2019.
- [28] Z. Yuan, A. W. Hall, S. Zhou, L. Brunke, M. Greeff, J. Panerati, and A. P. Schoellig, "Safe-control-gym: A unified benchmark suite for safe learning-based control and reinforcement learning in robotics," *IEEE Robotics and Automation Letters*, vol. 7, no. 4, pp. 11 142–11 149, 2022.
- [29] S. Ha, P. Xu, Z. Tan, S. Levine, and J. Tan, "Learning to walk in the real world with minimal human effort," in *Conference on Robot Learning*. PMLR, 2021, pp. 1110–1120.
- [30] G. Brockman, V. Cheung, L. Pettersson, J. Schneider, J. Schulman, J. Tang, and W. Zaremba, "Openai gym," *arXiv preprint arXiv:1606.01540*, 2016.



Yujie Yang Yujie Yang received his B.S. degree in automotive engineering from the School of Vehicle and Mobility, Tsinghua University, Beijing, China, in 2021. He is currently pursuing his Ph.D. degree in the School of Vehicle and Mobility, Tsinghua University, Beijing, China. His research interests include decision and control of autonomous vehicles and safe reinforcement learning.



Zhilong Zheng Zhilong Zheng received his B.S. degree in automotive engineering from the School of Vehicle and Mobility, Tsinghua University, Beijing, China, in 2022. He is currently pursuing his Ph.D. degree in the School of Vehicle and Mobility, Tsinghua University, Beijing, China. His research interests include decision and control of autonomous vehicles and safe reinforcement learning.



Xianyuan Zhan Dr. Xianyuan Zhan is an assistant professor at the Institute for AI Industry Research (AIR), Tsinghua University. He received a dual Master's degree in Computer Science and Transportation Engineering, and a PhD degree in Transportation Engineering from Purdue University. Before joining AIR, Dr. Zhan was a data scientist at JD Technology and also a researcher at Microsoft Research Asia (MSRA). His research interests include data-driven decision-making and urban computing. He has published more than 50 papers in top conferences and journals in the field of Computer Science and Transportation Engineering.



Shengbo Eben Li Shengbo Eben Li received his M.S. and Ph.D. degrees from Tsinghua University in 2006 and 2009. Before joining Tsinghua University, he has worked at Stanford University, University of Michigan, and UC Berkeley. His active research interests include intelligent vehicles and driver assistance, deep reinforcement learning, optimal control and estimation, etc. He is the author of over 130 peer-reviewed journal/conference papers, and the co-inventor of over 30 patents. He is the recipient

of the best (student) paper awards of IEEE ITSC, ICCAS, IEEE ICUS, CCCC, etc. His important awards include National Award for Technological Invention of China (2013), Excellent Young Scholar of NSF China (2016), Young Professor of ChangJiang Scholar Program (2016), National Award for Progress in Sci & Tech of China (2018), Distinguished Young Scholar of Beijing NSF (2018), Youth Sci & Tech Innovation Leader from MOST (2020), etc. He also serves as Board of Governor of IEEE ITS Society, Senior AE of IEEE OJ ITS, and AEs of IEEE ITSM, IEEE Trans ITS, Automotive Innovation, etc.



Jingliang Duan Jingliang Duan received his doctoral degree in mechanical engineering from the School of Vehicle and Mobility at Tsinghua University, China, in 2021. In 2019, he spent time as a visiting student researcher in the Department of Mechanical Engineering at the University of California, Berkeley. Following his Ph.D., he served as a research fellow in the Department of Electrical and Computer Engineering at the National University of Singapore from 2021 to 2022. He is currently a tenured associate professor in the School of Mechanical Engineering, University of Science and Technology Beijing, China. His research interests include reinforcement learning, optimal control, and self-driving decision-making.

professor in the School of Mechanical Engineering, University of Science and Technology Beijing, China. His research interests include reinforcement learning, optimal control, and self-driving decision-making.



Jingjing Liu Dr. Jingjing Liu is Professor, Principal Investigator at Tsinghua University. Her current research interests span from Multimodal AI and Self-supervised Learning to Reinforcement Learning and AI for Science. Dr. Liu has published 90+ papers at top AI conferences and journals (NeurIPS, ICML, CVPR, ACL, etc.) with 10K+ citations, and has received the Best Student Paper Honorable Mention Awards at CVPR and WACV. Before joining Tsinghua University in 2021, Dr. Liu was Senior Principal Research

Manager at Microsoft in Redmond, US, leading a research group on Vision-Language Multimodal AI. Prior to joining Microsoft Research, Dr. Liu was Research Scientist at MIT CSAIL in Cambridge, US, with the research focus on Spoken Dialogue Systems. Dr. Liu received the PhD degree in Computer Science from MIT EECS. She also holds an MBA degree from Judge Business School (JBS) at University of Cambridge in the UK.



Ya-Qin Zhang Dr. Ya-Qin Zhang is Chair Professor of AI Science at Tsinghua University, and Dean of Institute for AI Industry Research of Tsinghua University (AIR). He was the President of Baidu Inc. from 2014 to 2019. Prior to Baidu, Dr. Zhang was a Microsoft executive for 16 years with different key positions, including Managing Director of Microsoft Research Asia, Chairman of Microsoft China, and Corporate Vice President and Chairman of Microsoft Asia R&D.

Dr. Zhang was elected to the Chinese Academy of Engineering (CAE), the American Academy of Arts and Sciences (AAA&S), the Australian Academy of Engineering (ATSE), the National Academy of Inventors (NAI), and the Euro-Asia Academy of Sciences. He is a Fellow of IEEE and CAAI. He is one of the top scientists and technologists in digital video and AI, with over 500 papers, 60 granted US patents, and 11 books. His original research has become the basis for start-up ventures, new products, and international standards in digital video, cloud computing, and autonomous driving.

He serves on the Board of Directors of four public companies. He is on the industry board of United Nation Development Program (UNDP), and AI global council of the Davos World Economic Forum. He is the Chairman of world's largest open autonomous driving platform "Apollo" alliance with over 200 global partners. He has been an active speaker in global forums including APEC, Davos, United Nations, and Bo'Ao Asia Forum.

APPENDIX A

DETAILS OF CLASSIC CONTROL TASKS

In order to avoid confusion in symbols, in this section, we mark the states and actions in bold to emphasize that they are vectors.

A.1 ACC

In ACC, a following vehicle tries to converge to and maintain a fixed distance with respect to a leading vehicle moving in a uniform motion. Both following and leading vehicles are modeled as point masses moving in a straight line. The dynamics of the system is

$$\begin{pmatrix} \dot{x}_1 \\ \dot{x}_2 \end{pmatrix} = \begin{pmatrix} x_2 \\ 0 \end{pmatrix} + \begin{pmatrix} 0 \\ -1 \end{pmatrix} \mathbf{u}, \quad (22)$$

where $\mathbf{x} = [x_1, x_2]^\top \triangleq [\Delta s, \Delta v]^\top$, with $\Delta s = s - s_0$ standing for the difference between actual distance s and expected distance s_0 between the two vehicles and Δv standing for the relative velocity. The action $\mathbf{u} \triangleq [a]$ is the acceleration of the following vehicle.

The reward function is defined as

$$r(\mathbf{x}, \mathbf{u}) = -0.001\Delta s^2 - 0.01\Delta v^2 - a^2, \quad (23)$$

and the constraint function is

$$h(\mathbf{x}) = |\Delta s| - \Delta s_{\max}, \quad (24)$$

which, since a large acceleration is penalized in (23), will be violated by a performance-only policy.

A.2 LK

The goal of LK is to keep a vehicle running in a straight line. The state of the vehicle $\mathbf{x} \triangleq [y, \varphi, v, \omega]^\top$ includes y the vertical position, φ the yaw angle, v the lateral velocity and ω the yaw rate. The vehicle follows a 2-Degree-of-Freedom (DoF) bicycle model, where its longitudinal velocity is a constant, and the only action is steering angle, i.e. $\mathbf{u} \triangleq [\delta]$.

The reward function penalizes stabilization errors and aggressive behaviour:

$$r(\mathbf{x}, \mathbf{u}) = -0.01y^2 - 0.01\varphi^2 - v^2 - \omega^2 - \delta^2, \quad (25)$$

and the constraint function is

$$h(\mathbf{x}) = |y| - L/2, \quad (26)$$

where L is the width of the lane.

A.3 Pendulum

This task comes from the popular benchmark Gymnasium [30], with some slight changes. The state $\mathbf{x} \triangleq [\theta, \dot{\theta}]^\top$ consists of the pendulum's angle w.r.t. vertical θ and angular velocity $\dot{\theta}$ and the action is $\mathbf{u} \triangleq [\tau]$, representing the torque applied on the fixed end of the pendulum. Different to the Gymnasium version, the reward function is changed to

$$r(\mathbf{x}, \mathbf{u}) = -0.1\theta^2 - 0.01\dot{\theta}^2 - \tau^2, \quad (27)$$

and an additional constraint

$$h(\mathbf{x}) = |\theta| - \theta_{\max} \leq 0 \quad (28)$$

is imposed on the angle.

A.4 Quadrotor

In the Quadrotor, a 2D quadrotor is required to follow a circular trajectory in the vertical plane while keeping the vertical position in a certain range. The state of the system is $\mathbf{x} \triangleq [x, \dot{x}, z, \dot{z}, \theta, \dot{\theta}]^\top$, where (x, z) is the position of the quadrotor on xz -plane, and θ is the pitch angle. The action of the system is $\mathbf{u} \triangleq [T_1, T_2]^\top$, including the thrusts generated by two pairs of motors.

The goal is to minimize the tracking error with minimal efforts:

$$\begin{aligned} r(\mathbf{x}, \mathbf{u}) = & -\|[\mathbf{x} - \mathbf{x}_{\text{ref}}, \mathbf{z} - \mathbf{z}_{\text{ref}}]\|_2^2 \\ & - 0.1\theta^2 - \dot{\theta}^2 \\ & - 0.1(T_1 - T_0)^2 - 0.1(T_2 - T_0)^2, \end{aligned} \quad (29)$$

where $(\mathbf{x}_{\text{ref}}, \mathbf{z}_{\text{ref}})$ is the reference position the quadrotor is supposed to be at, and T_0 is the thrust needed for balancing the gravity. The reference position moves along a circle $x^2 + z^2 = 0.5^2$ with a constant angular velocity, but the constraint function is

$$h(\mathbf{x}) = \begin{bmatrix} |z| - z_{\max} \\ |\theta| - \theta_{\max} \\ \|[\mathbf{x} - \mathbf{x}_{\text{ref}}, \mathbf{z} - \mathbf{z}_{\text{ref}}]\|_2 - \text{err}_{\max} \end{bmatrix} \leq 0, \quad (30)$$

restricting the quadrotor to stay in a rectangular area.

APPENDIX B

HANDCRAFTED CBFS

The control barrier function $B(\mathbf{x}) : \mathcal{X} \rightarrow \mathbb{R}$ for ACC is

$$B(\mathbf{x}) = \begin{cases} -10 + \Delta s + 4.5\Delta v & \Delta v \geq 0 \\ -10 - \Delta s - 3.2\Delta v & \Delta v < 0 \end{cases}. \quad (31)$$

The control barrier function for LK is

$$B(\mathbf{x}) = \begin{cases} -L/2 + 1.8y + 3.2\varphi^2 + 0.5v + 0.8\omega & \phi \geq 0 \\ -L/2 - 1.8y - 3.2\varphi^2 - 0.5v - 0.8\omega & \phi < 0 \end{cases}. \quad (32)$$

The control barrier function for Pendulum is

$$B(\mathbf{x}) = \begin{cases} -\theta_{\max} + \theta + 0.3\dot{\theta} & \dot{\theta} \geq 0 \\ -\theta_{\max} - \theta - 0.3\dot{\theta} & \dot{\theta} < 0 \end{cases}. \quad (33)$$

The control barrier function for the Quadrotor is

$$\begin{aligned} B(\mathbf{x}) = & -z_{\max} + 2.35z^2 \\ & + \begin{cases} 2\text{err}^2 + 0.2\dot{z} & 0 \leq z \leq z_{\max} \\ 2\text{err}^2 - 0.2\dot{z} & -z_{\max} \leq z < 0, \\ 2\text{err}^2 & \text{others} \end{cases} \end{aligned} \quad (34)$$

where $\text{err} = \|[\mathbf{x} - \mathbf{x}_{\text{ref}}, \mathbf{z} - \mathbf{z}_{\text{ref}}]\|_2$.

The control barrier function for Safety Gym environments is

$$B(\mathbf{x}) = r - d - 0.3\dot{d}, \quad (35)$$

where r is the radius of hazards and d is the distance to the center of the nearest hazard.

With a control barrier function, the constraint is constructed as $B(f(\mathbf{x}, \mathbf{u})) - B(\mathbf{x}) \leq -\lambda B(\mathbf{x})$.

APPENDIX C

HYPERPARAMETERS

The hyperparameters used in the experiments are listed in Table 2 and Table 3.

TABLE 2
Hyperparameters of the off-policy algorithms

Hyperparameter	Value	
	Classic	Safety Gym
<i>Shared</i>		
Discount factor	0.99	
Number of hidden layers	2	
Number of hidden neurons	256	
Optimizer	Adam($\beta_1=0.99, \beta_2=0.999$)	
<i>SAC-related</i>		
Activation function	ReLU	
Target entropy	$-\dim(\mathcal{U})$	
Initial temperature	1.0	
Target smoothing coefficient	0.005	
Learning rate	1e-4	
Batch size	256	1024
Replay buffer size	2×10^6	4×10^6
<i>Lagrange-related</i>		
Initial Lagrange multiplier	1.0	
Multiplier learning rate	1e-4	
Multiplier delay	10	
<i>CBF-related</i>		
λ	0.1	
<i>FPI-related (ours)</i>		
Feasibility threshold (p)	0.1	
Initial t	1.0	
t increase factor	1.1	
t update delay	10000	

TABLE 3
Hyperparameters of the on-policy algorithms

Hyperparameter	Value	
	Classic	Safety Gym
<i>Shared</i>		
Discount factor	0.99	
Number of hidden layers	2	
Number of hidden neurons	256	
Activation function	Tanh	
Optimizer	Adam($\beta_1=0.99, \beta_2=0.999$)	
GAE parameter	0.97	
Target KL divergence	0.01	
Batch size	4000	10000
Number of epochs	500	400
<i>CPO-related</i>		
Number of actors	10	
Learning rate	1e-3	
Number of critic updates per iteration	80	
Backtrack coefficient	0.8	
Backtrack iterations	10	
<i>PPO-related</i>		
Learning rate	1e-4	
Number of actors	20	10
Horizon	200	1000
SGD minibatch size	200	500
Number of SGD steps per epoch	30	
<i>Lagrange-related</i>		
Initial Lagrange multiplier	1.0	
Multiplier learning rate	0.05	
Multiplier delay	1	